HHS Public Access

Author manuscript

Epidemics. Author manuscript; available in PMC 2020 January 13.

Published in final edited form as:

Epidemics. 2019 September ; 28: 100348. doi:10.1016/j.epidem.2019.100348.

School dismissal as a pandemic influenza response: When, where and for how long?

Timothy C. Germann[a], **Hongjiang Gao**[b,*], **Manoj Gambhir**[c,d,1], **Andrew Plummer**[b,2], **Matthew Biggerstaff**[c], **Carrie Reed**[c], **Amra Uzicanin**[b]

[a]Theoretical Division, Los Alamos National Laboratory, Los Alamos, NM 87545 USA

[b]Community Interventions for Infection Control Unit, Centers for Disease Control and Prevention, Atlanta, GA 30329 USA

[c]National Center for Immunization and Respiratory Diseases, Centers for Disease Control and Prevention, Atlanta, GA 30333 USA

[d]School of Public Health and Preventive Medicine, Monash University, Victoria 3800 Australia

Abstract

We used individual-based computer simulation models at community, regional and national levels to evaluate the likely impact of coordinated pre-emptive school dismissal policies during an influenza pandemic. Such policies involve three key decisions: when, over what geographical scale, and how long to keep schools closed. Our evaluation includes uncertainty and sensitivity analyses, as well as model output uncertainties arising from variability in serial intervals and presumed modifications of social contacts during school dismissal periods. During the period before vaccines become widely available, school dismissals are particularly effective in delaying the epidemic peak, typically by 4–6 days for each additional week of dismissal. Assuming the surveillance is able to correctly and promptly diagnose at least 5–10% of symptomatic individuals within the jurisdiction, dismissals at the city or county level yield the greatest reduction in disease incidence for a given dismissal duration for all but the most severe pandemic scenarios considered here. Broader (multi-county) dismissals should be considered for the most severe and fast-spreading (1918-like) pandemics, in which multi-month closures may be necessary to delay the epidemic peak sufficiently to allow for vaccines to be implemented.

Keywords

Pandemic influenza; School dismissal; Stochastic individual-based model; EpiCast

*Corresponding author. hgao@cdc.gov (H. Gao).

[1]Present address: IBM Health Modeling and Analytics Melbourne Research Laboratory, Melbourne, Victoria 3006 Australia.

[2]Present address: TRICARE/Defense Health Agency, Reston, VA 20190 USA.

Disclaimer

The findings and conclusions in this report are those of the authors and do not necessarily represent the official position of the Centers for Disease Control and Prevention.

Appendix A. Supplementary data

Supplementary material related to this article can be found, in the online version, at doi: https://doi.org/10.1016/j.epidem.2019.100348.

1. Introduction

Influenza pandemics occur when a novel influenza virus gains sustained human-to-human transmission and spreads globally, resulting in potentially high levels of morbidity and/or mortality. Following the emergence of a novel pandemic strain, several months are typically required to develop, produce, and distribute a well-matched pandemic vaccine (Gerdil, 2003; Centers for Disease Control and Prevention, 2010; President's Council of Advisors on Science and Technology, 2010). Moreover, the use of antiviral drugs for chemoprophylaxis may be limited due to concerns regarding drug resistance and limited supply during an evolving pandemic (Lipsitch et al., 2007; Centers for Disease Control and Prevention, 2011). As a result, non-pharmaceutical interventions (NPIs) are essential, potentially providing time for pandemic vaccines to be developed and distributed, decreasing the peak demand for healthcare services prior to pandemic vaccine roll-out, and reducing the overall morbidity and mortality caused by the novel virus. Among potential NPIs, school closure/dismissal has long been one of the first to be implemented during previous pandemics (Markel et al., 2007a; Cauchemez et al., 2009), given the major role that school-aged children play in the transmission of influenza in the household (Longini et al., 1982; Viboud et al., 2004) and community (Chao et al., 2010), likely due to intense social contacts among children in schools (Mossong et al., 2008).

In the absence of clear evidence for the effectiveness of school closures on large geographic scales, it has been very difficult for public officials to make policy recommendations and develop national guidance. Mathematical and computational disease spread models offer invaluable platforms for performing "what-if" studies to assess potential future pandemic scenarios and intervention strategies, complementing observational or field studies that are necessarily limited to historical events and decisions (Germann et al., 2006; Halloran et al., 2008). In particular, they enable us to model a variety of school dismissal strategies and assess their effectiveness in slowing the spread of a hypothetical future influenza pandemic (Haber et al., 2007; Milne et al., 2008; Halder et al., 2010; Lee et al., 2010; Halder et al., 2011; Brown et al., 2011; Milne et al., 2013; Nishiura et al., 2014; Fung et al., 2015). However, previous pre-pandemic policy recommendations used a measure of pandemic severity that was based on disease severity measures, such as case fatality ratio and excess death rate (Centers for Disease Control and Prevention, 2007), while modeling studies primarily considered the effectiveness of school dismissal strategies for various disease transmissibility levels, usually represented by the basic reproduction number R0 (Germann et al., 2006; Halloran et al., 2008; Harber et al., 2007; Milne et al., 2008; Halder et al., 2010; Lee et al., 2010; Halder et al., 2011; Brown et al., 2011; Milne et al., 2013; Nishiura et al., 2014; Fung et al., 2015). A recently developed two-dimensional pandemic severity assessment framework considers both transmissibility and clinical severity as two independent factors (Reed et al., 2013). This framework provides the basis for the development of national pre-pandemic NPI guidance, for which school closure is thought to be one of the most effective early mitigation measures. The purpose of the present study is to evaluate whether school dismissal should be recommended and, if so, when such dismissals should be initiated, how broadly (in geographic terms, e.g., community, county, or state-wide dismissals), and how long they should last. As described in the Methods, we

utilize simulations at three different scales to answer these questions in a computationally feasible manner. A single community model (~2000 people) is used for sensitivity studies, and a regional model (~8.6 million people in the Chicago metropolitan area) to address timing ("when" and "how long") and local vs. regional dismissal policies. The insights gleaned from these smaller-scale simulations are then used to design the final simulation suite, employing a model of the continental United States (~300 million people).

2. Methods

2.1. Simulation platform

In the present work, we extend and apply the stochastic, individual-based EpiCast ("Epidemiological Forecasting") model (Germann et al., 2006; Halloran et al., 2008) to evaluate a range of school dismissal policy options for five potential influenza pandemic strains having characteristics based upon both historical (1918, 1957, 1968, and 2009) and potential H5N1-like pandemics, spanning the four quadrants (with independent severity and transmissibility axes) of the pandemic severity assessment framework (Reed et al., 2013). Full details about EpiCast are provided in the SI.

2.2. Model parameters and assumptions

For each of these five pandemic scenarios and three geographical scales, four other parameters are varied (see Table 1) in order to span their likely ranges and ascertain their impact on mitigation. First, we consider two alternative disease natural histories ("Short" and "Long"), with serial intervals (average time between successive cases) of ~2.8 and 4 days, respectively. These two choices have been used in several previous modeling studies (Halloran et al., 2008), and almost exactly span the 95% confidence interval of 2.9–4.3 days observed in a household study during the 2007 interpandemic influenza season in Hong Kong (Cowling et al., 2009)

Second, we considered different triggers for school dismissal, all involving the diagnosis of some threshold number of symptomatic school children within a community. Once that threshold is reached, all schools within that community are closed, and possibly those in surrounding communities, depending upon the specific policy. Since it will be impossible to quickly identify and accurately diagnose all symptomatic children, the surveillance sensitivity is an important factor. In the present study, no other actions (e.g., therapeutic antivirals, isolation, or quarantine) other than self-isolation (staying home when sick, as specified in SI section 1 F) are taken following diagnosis. Consequently, the diagnosis ratio (the percentage of newly symptomatic individuals correctly and promptly identified following illness onset) and the trigger threshold (the number of diagnosed school children required to activate a dismissal) can be coupled to provide a single independent parameter for the trigger, the number of symptomatic (but not necessarily diagnosed) school children. For example, if the diagnosis of a single child is sufficient to trigger intervention, then diagnosis ratios of 1%, 5%, 10%, and 20% require 100, 20, 10, and five symptomatic school children, respectively, in a community before the first symptomatic child is diagnosed, triggering the intervention.

Third, the geographic scale of school dismissal can range from the individual community (which may be considered as a very small ~2000-person school district), to single county, multi-county, or even potentially state- or nation-wide closures in the most severe situation, as in the 1918-like scenario D. With the regional model, we consider school dismissal at either the individual community or region-wide levels, and at the national scale consider four scales of dismissal: community, county, adjoining county region, or (for the 1918-like scenario D only) state-wide dismissals.

Finally, in the face of a limited amount of survey and field study data on social contact behaviors in and out of school from the United States (Mossong et al., 2008; Gog et al., 2014; Earn et al., 2012; Copeland et al., 2013; Chowell et al., 2011; Heymann et al., 2004; Markel et al., 2007; Eames et al., 2012), we utilize a range of assumed social contact pattern changes during school dismissal that is consistent with the available studies and span those used in previous modeling work (Germann et al., 2006; Halloran et al., 2008; Haber et al., 2007; Milne et al., 2008; Halder et al., 2010; Lee et al., 2010; Halder et al., 2011; Brown et al., 2011; Milne et al., 2013; Nishiura et al., 2014; Fung et al., 2015). Since these contact rates contribute to the infection probability for each susceptible person, they have a strong influence on overall disease transmission, and unrealistic assumptions (e.g., “no contacts between children during school dismissal”) can lead to overly optimistic expectations for the benefits of school dismissal. To provide likely bounds on the effectiveness of school dismissal policies for each combination of school dismissal policy and pandemic scenario, we consider two assumptions, representing either a “worst-case” (with a greater amount of contact during closure, in which household contacts involving children are doubled, and child-related contacts outside the home are reduced by only 30%) and a “best-case” (with no change in household contacts and a 50% reduction in outside contacts) scenario. In both cases, all schools, preschools, daycares, and playgroups within the affected community (or communities) are closed during dismissal, so no transmission occurs within these mixing groups. Social contact surveys (Eames et al., 2012) and mathematical model-based analysis of virological data (Earn et al., 2012) during the 2009 summer and fall holiday breaks suggest that there is a reduction of at least 40–50% in contact and transmission among school-age children during such regularly scheduled dismissals; pre-emptive coordinated school dismissals undertaken as a countermeasure during an evolving pandemic would likely lead to additional precautions, reducing contacts even further.

We also assume that a well-matched vaccine will be available 6 months after the first U.S. index case. The assumed vaccine efficacy for susceptibility VEs = 0.70 (VEs = 0.50 for age 65+) represents the reduced susceptibility to infection and influenza illness of vaccinated individuals, while the vaccine efficacy for infectiousness VEi = 0.80 (for all age groups) represents the reduced infectiousness to others (Longini et al., 2000). Full details about vaccine assumption are described in the SI. To separate the effects of school dismissal alone from that coupled with a vaccination campaign, we will measure cumulative attack rates both before (on day 180) and after (on day 240) vaccine introduction.

2.3. Sensitivity analysis

A model of a single community of 2000 persons is used to identify the key model parameters and quantify their impact on the mitigation of disease spread (Blower and Dowlatabadi, 1994). We consider six contact settings: households, household clusters, neighborhoods, communities, schools, and workplaces. Latin hypercube sampling is used to sample the contact probability in each setting, then partial rank correlation coefficients are calculated as the outcome measure for sensitivity analysis. Full details are presented in the SI.

2.4. Model parameter calibration

The model of a small community was also used to develop an initial set of model parameters for each of the five pandemic scenarios under consideration (Table 1). The specified age-specific attack-rate patterns, basic reproduction number R0, and case fatality ratios were fit by adjusting the baseline EpiCast model contact rates (Germann et al., 2006) to give age-specific and overall attack rates within 1% of the specified values. For instance, in order to increase the childhood attack rate, the corresponding school contact rate is increased. Similarly, to increase the working-age adult attack rate, the workplace contact rate is raised.

2.5. Scoping studies

The regional (Chicago-area) model was used for an earlier study involving EpiCast and two other individual-based, stochastic simulation models (Halloran et al., 2008). Here, we use it for scoping studies to evaluate the impact of the trigger and duration of school dismissal, which will then be used to down-select to a smaller number of scenarios to be evaluated using the more computationally expensive national-scale model. The baseline parameters for each pandemic scenario are adjusted slightly from their single-community values (reflecting the more dispersed and heterogeneous population structure of the larger-scale model), giving the model parameters listed in Table S1 and baseline epidemic curves shown in Fig. S2. School dismissal options are then systematically studied by considering all possible combinations of the model parameters listed in Table 1. With regard to the geographic scale, this model considers either community-by-community or simultaneous region-wide school dismissals. Furthermore, for the most severe and transmissible 1918-like scenario D, longer durations of closure (e.g., 16–24 weeks) are also explored.

2.6. National-scale simulation studies

For simulations of pandemic spread across the continental United States, the manner of introduction of a pandemic influenza strain must be considered. In particular, a human-transmissible strain may emerge either domestically or overseas, in both cases most likely in a rural area. As discussed in the SI, the subsequent epidemic will slowly spread through the more dispersed rural population before reaching a dense urban population where it can thrive, and it is during this early, rural, spread, whether in the U.S. or overseas, that early characterization and vaccine development can begin. One plausible domestic emergence scenario is modeled by the introduction of 10 infected individuals into Sussex County, Delaware, a large poultry-farming region on the Delaware-Maryland-Virginia (DelMarVa) peninsula. Previous studies (Germann et al., 2006) have found that introduction via air

travel into major metropolitan areas, or point source introductions into large cities (either New York or Los Angeles), result in nearly identical national-level incidence rates, with only a difference in the details of the spatiotemporal spread. Consequently, we assume an introduction via arriving international air passengers (2 per 10,000) for this overseas scenario, a rate comparable with that used for the regional model.

Given the greatly increased computational cost of the national-scale model, the comprehensive set of regional model results is used to identify the most useful set of larger-scale simulations. As the two scenarios with the highest clinical severity and the least and most transmissible spread, pandemic scenarios C and D are both included in the national-scale study. School dismissal is unlikely to be invoked for the low-transmissibility, low-severity scenario A, so it is not considered further. While there are subtle differences in results for scenarios B1 and B2, we focus on B2 due to its higher severity and transmissibility than B1. We consider three geographic scales of school dismissal for each of these scenarios: community, county, multi-county region (including the affected county and all immediately adjacent counties), and additionally a coordinated (simultaneous) state-wide dismissal for the worst-case scenario D.

3. Results

3.1. Single community model

By attributing each new infection to a single source based on relative contributions of contacts to the overall transmission probability, we find that household transmission dominates (˜40%), followed by the age-appropriate daytime mixing group (school or work) (˜30%) and non-specific contact settings (also ˜30%), both for the original contact parameters and for the modified contact parameters calibrated for the five pandemic scenarios (Fig. S3 in the Supplementary information (SI)). This is consistent with the pattern used in other modeling work, with perhaps a slightly increased household transmission. In accord with this finding, sensitivity analyses performed on the single-community model confirm that the assumed household, school, and workplace contacts (in that order) have the greatest impact on the resulting cumulative attack rate, with non-specific community transmission (which contributes to roughly a quarter of all cases) following closely behind. The relationship between these contact matrix elements and the epidemic timing is even more interesting. The partial rank correlation coefficient (PRCC) shown in Fig. S4, which measures the sensitivity of output variables to inputs, indicates that school transmission has, by far, the largest impact on the number of days from initial outbreak to peak incidence (a PRCC of −0.55), followed by household transmission (−0.27) (The negative values simply indicate that for *increasing* contact rates, the time to peak incidence *decreases*.). Interestingly, the workplace contact rate PRCC (+0.11) has the opposite (positive) sign, but its small magnitude may indicate that this is merely a statistical fluke.

3.2. Regional model

The impacts of school dismissal policies for the regional model are summarized in Table 2, which presents the cumulative attack rate (averaged over five stochastic realizations) and its reduction from its baseline value (without any school dismissal) under each simulation

scenario. The results in Table 2 are for a shorter serial interval and "best-case" contact rates (i.e., the least plausible amount of person-to-person contact) during school dismissal (see Methods); corresponding tables for the longer serial interval and/or worst-case contact patterns are provided in the SI, Tables S2–S4. From Table 2, if we compare community-wide and region-wide school dismissals of the same duration, pandemic scenarios and diagnosis ratio, the reductions of overall clinical attack rate for community-wide closures are usually higher than for region-wide closures for pandemic scenarios A, B1, B2, and D (see Methods for a description of pandemic scenarios). In pandemic scenario C, with longer school dismissals (> 4 weeks), region-wide dismissals most often have a greater attack rate reduction than the community-wide closures. Similar trends are observed whether the cumulative incidence is measured before (at day 180, Tables S5–S8) or after (at day 240, Tables 2 and S2–S4) the onset of an assumed vaccination campaign, particularly for the more transmissible scenarios B2 and D. Consequently, we will limit our subsequent discussion to the post-vaccination results based on the full 240-day simulation.

Further insight is provided by the epidemic curves for different dismissal scenarios, such as those shown in Fig. 1 for the region-wide dismissal, shorter serial interval, worst-case contact patterns, and trigger of 20 symptomatic children (i.e., dismissal upon the first diagnosed case for a 5% diagnosis ratio). Here we can see that the primary benefit of dismissals are to delay the epidemic peak, by 5–6 days per week of dismissal for most pandemic scenarios, until the peak is postponed long enough for vaccines to be introduced and reduce the spread. These delays are comparable with the ˜5 days per week of dismissal recently found with a compartmental model for more severe epidemics (with a 30% baseline attack rate) (Fung et al., 2015). For the mildest pandemic scenario C, the spread is so slow and the peak so late that it is only delayed by 3–4 days per week of dismissal.

3.3. National model

For national-scale simulations, different manners of introduction of the pandemic influenza strain resulted in different disease spread dynamics. For instance, the emergence of a domestic strain from a rural area in the U.S. would likely take longer to result in widespread transmission than the importation of a novel virus from overseas which was already spreading from human to human before arriving at an urban area (where international airports are located) in the U.S. (see Figs. S7 and S8 in the SI). In addition to this, our simulation indicated that emergence of a domestic strain in a rural area had a finite probability of extinction, and its peak transmission may lag behind 1–3 months compared to that of a novel virus introduction into an urban area. For these reasons, we focus hereinafter on the results from the national-scale models that assume an overseas emergence of the novel virus with entry into the United States via air travel.

National-scale model outcomes, in terms of (symptomatic) cases averted for two pandemic scenarios (B2 and D) for different dismissal triggers, durations, and geographic scales, are presented in Fig. 2. A different view of the impacts of varying spatial extent of school dismissal is shown in Fig. 3 for pandemic scenarios B2 and D, with a 4-week closure after 20 symptomatic children appear in a community (i.e., dismissing schools upon the first detected child at a 5% diagnosis ratio). Epidemic curves are compared in the top panels

for the two considered contact rate changes upon school dismissal. In the bottom panels, we show the number of schools closed over time. (These results are for the worst-case contact-rate assumption; those for the best-care contact rates are shown in Fig. S6.) As shown in Figs. S9 and S10, the reduced transmissibility of scenario C, combined with the slower spread across the dispersed U.S. population, causes it to have not yet reached its epidemic peak by the assumed availability date of an effective vaccine, six months after the first introduction. As subsequent vaccination slows and ultimately stamps out the outbreak, the effect of vaccination dominates the impact of any school dismissal and precludes any further consideration of this scenario for the national-scale model.

From Fig. 3, we observe that community-wide school dismissals reduce the peak incidence without significantly delaying the time-to-peak incidence. On the other hand, multi-county and state-wide school dismissals have more impact on delaying the time-to-peak than reducing the peak incidence. Furthermore, county-wide school dismissals have a similar time-to-epidemic-peak as multi-county and state-wide school dismissals, but with a lower peak incidence than either. These results (Fig. 2) for the effectiveness of community-wide school-dis- missal strategies are consistent with the results for the regional model (see Table 2). In particular, for a low (but plausible) diagnosis ratio of 1%, waiting to close individual schools until even the first detected case may never occur. Efficacy increases with both the diagnosis ratio and duration, although a diminishing return is observed for longer dismissal durations, in particular the extended 16- and 20-week durations for scenario D. However, the chief advantage of the national-scale model is that it allows us to explore varying geographic scales of school dismissal. We find that the optimal geographic scale of school dismissal depends on the duration and trigger/diagnosis ratio (see Fig. 2). More proactive dismissals (i.e., those over broader geographic regions) are only advantageous if the closure is sufficiently long to enable vaccination, which often means a month or longer dismissal. Additionally, more proactive school dismissals over a larger geographic area (multi-county, or state level) will be more appropriate (and effective, see Fig. 2) for settings where influenza surveillance is less sensitive (i.e., where the diagnosis ratio is likely to be low).

3.4. Observations

From these regional and national model results, several observations can be made. First, the main effect of school dismissals across wider geographic scales is to slow the spread of the virus, as reflected by delayed time-to-peak, which confers multiple benefits. One is to delay and reduce peak demand for healthcare, which is particularly important at the start of a pandemic when systems are not yet prepared to deal with an ever-increasing patient load. An even greater benefit is achieved if this delay extends sufficiently long for an effective vaccine to be developed, produced, and distributed to the population (see Fig. 3). Second, the effects of school closure are very sensitive to the ability of the local surveillance system to detect influenza circulation and, in turn, provide a “trigger” for closing schools. For a diagnosis ratio as low as 1%, which might occur if laboratory confirmation is required (Reed et al., 2009), dismissals may not be triggered in time and, thus, will have no effect on morbidity (see Table 2). In contrast, when surveillance systems are able to detect 5% or more influenza cases in the community, school closures of any duration and on any scale start reducing

cumulative incidence, with the effect being particularly prominent for closures lasting 8 weeks or longer (see Fig. 2).

Finally, school closures for shorter duration of closure (1–4 weeks) generally result in a greater number of cases averted at the local community level, compared to simultaneous school closures of the same duration implemented over a larger geographic area (county, multi-county, or state [see Fig. 2]). However, such simultaneous (coordinated) school closures proactively implemented over a wider region are usually superior in terms of number of cases averted if the closure is sustained over a longer period of time (8 weeks or more [see Fig. 2]). In addition, simultaneous (proactive) school dismissal policies more effectively delay the spread of the disease compared to the community-wide school closures of the same duration, albeit at the greater cost to society due to the larger number of schools that must remain closed than if the closures were implemented on an individual community-by-community basis (see bottom panels of Fig. 3). By primarily slowing, rather than reducing, the disease spread, such closures are capable of reducing the peak burden significantly if the delay extends into the time window when vaccines become available. In contrast, individual school dismissals do not have a substantial impact on when the peak burden is reached, but if implemented promptly after the occurrence of a few initial cases within a school or school district, they may help reduce its magnitude and, thus, the transitory surge on the healthcare system (see top panels of Fig. 3).

4. Discussion

The primary benefit of pre-emptive school dismissals in mitigating the spread of a novel influenza virus is the delayed time-to-peak that is seen in dismissals of any duration considered in our study, typically by 4–6 days for each week of dismissal. Delaying local outbreak peaks helps to decompress the demand on the healthcare system during the initial pandemic wave and, under certain circumstances, it may help “buy time” to prepare and roll out a pandemic vaccine. That the main effect of school dismissals is delaying the time-to-peak is fully consistent with the nature of an intervention that does not provide specific protection. Overall, longer pre-emptive school dismissals (≥4 weeks) implemented simultaneously on a wider geographic scale (e.g., county level or wider) are most impactful in mitigating an influenza pandemic in its early stages, while awaiting the production and distribution of a pandemic vaccine. However, as Fig. 1 indicates, for highly transmissible strains, it may be difficult to close schools long enough to delay the epidemic peak until vaccines become available. Thus, efforts to increase the speed of vaccine production and distribution are essential to ensure that the time bought by school dismissal yields the optimal benefit (Biggerstaff et al., 2015).

In addition to delaying the time-to-peak, school dismissals of sufficient duration implemented pre-emptively on a wide-enough geographic scale may also reduce the cumulative attack rate. Our results suggest that shorter precisely targeted dismissals (1–4 weeks) implemented on an individual community-by-community basis following detection of initial cases among students at these schools appear to be superior to dismissals of the same duration implemented in a coordinated county-wide, multi-county, or state-wide manner. However, such dismissals may not be feasible in practice, as precise targeting

requires prompt laboratory confirmation of initial cases in each and every community, coupled with quick dismissal of an affected school before virus spread occurs within the school and between the school and the surrounding community. For longer (multi-month) dismissals, we find that a greater reduction in cases is achieved by coordinated larger-scale dismissals (county-level or wider), being proactive rather than waiting until cases are detected in each individual community. Therefore, for the most severe pandemic scenarios, we believe that the optimal geographic unit for implementation of pre-emptive school closures as a pandemic countermeasure will be county-wide or beyond.

For less transmissible strains causing severe disease (e.g., a potential H5N1-like scenario) represented by the scenario C in our study, the effect of school dismissal on cumulative disease incidence is quite pronounced, even for shorter dismissals implemented on a narrower geographic scale. The already-low transmissibility (low R_0) in such a scenario provides an opportunity to achieve local extinction by strategically targeted and timed school closure following the initial local introduction even without vaccination. In contrast, for the most transmissible strains associated with a high clinical disease severity considered in our study (i.e., scenario D comparable to 1918), a significant reduction in cumulative disease incidence by school closure alone may only be possible when schools are out of session for 16 weeks or longer, at a county-wide or wider geographic scale. It should be noted, how- ever, that depending on the timing of the initial pandemic waves, the effect of a long continuous school dismissal (16+ weeks) may be realized through a combination of planned school holidays and an additional dismissal (or delayed start of a semester) in response to the pandemic.

These results highlight an important practical issue, namely that the effectiveness of school dismissals is highly dependent on the local surveillance systems' ability to quickly detect virus transmission in communities and, thus, implement (or "trigger") the intervention in a timely fashion. Delayed detection, associated with a less-sensitive surveillance method (e.g., by waiting for laboratory confirmation) results in a delayed implementation of the intervention and, thus, a diminished effect with regard to slowing down the transmission. For a low diagnosis ratio of 1%, delaying the closure of individual schools (or communities) until a child there is confirmed is a threshold that may never be reached. (For a 2000-person community in which 22% of the population is school-aged, there are only 440 school children; it is unlikely that 100 of them will be ill at the same time.) In these cases, more sensitive triggers or surveillance approaches may be needed to ensure school outbreaks are identified promptly. Interestingly, the opposite behavior is observed for simultaneous school dismissal. In that case, the greater risk is closing (and then reopening) schools too quickly before the epidemic reaches its peak. For a low diagnosis ratio, this is the only choice, and may be the most realistic in practice: if a school has so many affected students that it is forced to close, neighboring schools will benefit by proactively dismissing. In a way, the original school (which is unlikely to benefit from closing, since it may be too late) will serve as a sentinel event, signaling the impending risk of severity to surrounding communities. Given the extreme sensitivity of the effects of school dismissals to early detection of initial cases, an aggressive surveillance system, coupled with intense pre-pandemic planning for rapid implementation of community-based interventions such as school dis- missals, is needed in all settings. This may be particularly important in dense urban settings around

major international hubs, where introductions of novel influenza virus strains are most probable and where an extremely high population density may facilitate transmission of strains that may be less capable of circulating in more sparsely populated areas.

To our knowledge, this is the first study that systematically explored potential effects of school closures implemented on different geographic scales relevant for the U.S. (corresponding to local, county, regional/ state, and national governmental authorities) and in different pandemic severity scenarios.

Our findings are consistent with previously published studies considering school closures as the only intervention in response to an evolving pandemic. In particular, prior observational and modeling studies suggested that schools are the key community setting for pandemic influenza transmission (Chao et al., 2010; Gog et al., 2014). School closures have been found to be effective in slowing down influenza transmission, whether implemented as a mitigation strategy or due to other reasons (e.g., regular school breaks, teacher's strike, etc.) (Earn et al., 2012; Copeland et al., 2013; Chowell et al., 2011; Heymann et al., 2004; Markel et al., 2007). In addition, other modeling studies have explored school closure as a mitigation strategy (Halloran et al., 2008; Haber et al., 2007; Milne et al., 2008; Halder et al., 2010; Lee et al., 2010; Halder et al., 2011; Brown et al., 2011; Milne et al., 2013; Fumanelli et al., 2016; De LuCa et al., 2018). However, to our knowledge, ours is the most comprehensive modeling study to evaluate the effectiveness of different school-closure strategies – including the tradeoffs between local, regional, and national dismissals – in mitigating influenza in the United States during an evolving pandemic. Model adjustments and validation were undertaken to address the research question at hand using the best currently available empirical and observational data for model parameterization, and sensitivity analyses were used to test the robustness of key findings.

As has been comprehensively reviewed by (Riley 2007) and Carrasco et al (Carrasco et al., 2013), the great flexibility of such models is also their Achilles heel, as model developers, users, and consumers often construct models and parameters in data-poor (or data-free) environments. Intentionally (as is most always the case) or not, these decisions can lead to greater confidence in model predictions than may be warranted, given their typically tenuous tie to observed truth. However, although quantitative model predictions should generally be viewed with a healthy appreciation for their limitations, in many cases, qualitative trends have been proven to be reliable and useful in pre-pandemic planning efforts (Centers for Disease Control and Prevention, 2007). We have endeavored to consider and address the key limitations that are always present in mathematical modeling studies. In the present case, the greatest uncertainty concerns how contact rates (within different mixing groups and ages) might change during the disruption accompanying an unplanned school dismissal. These will presumably vary with time (as a so-called "fear-based social distancing" gradually decays towards normal contact rate patterns), and severity (e.g., the greater case fatality ratio of pandemic scenarios C and D are more likely to lead to a greater acceptance of, and compliance with, recommended social distancing measures. Currently, to our knowledge, there are no empirical data to inform how contact patterns may change during a prolonged closure; without such data, this limitation cannot be confidently addressed. On the disease side, there remains a great deal of variability and uncertainty about the natural history of

influenza, most notably its serial interval (we considered two possibilities which bracket the likely range) and the role of asymptomatic individuals in transmission (we have assumed 50% of all cases are asymptomatic; previous studies assume either 30% or 50%). As mentioned previously, the triggering of any mitigation measures is dependent upon a timely detection, while realistic diagnosis ratios for pandemic planning purposes remain uncertain (Biggerstaff et al., 2012).

In addition to testing the effects of school closures with regard to timing, duration, and geographic scale of their implementation during an evolving pandemic prior to vaccine rollout, we have performed several analyses to test the robustness of our key findings. A sensitivity and uncertainty analysis demonstrates that schools are the key community setting for influenza transmission, apart from households. Hence, reducing school transmission provides the greatest lever for slowing the disease spread before vaccination. While such analyses have rarely been performed for large, complex simulation models, many further questions remain for future research. For example, it would be important to explore to what extent the networking of multiple communities, as in our regional and national models, affects these parameter sensitivities and variability of outcomes through nonlinear effects. Since it is impossible to predict the precise characteristics of the next pandemic influenza strain, and the efficacy of potential pharmaceutical and non-pharmaceutical countermeasures, the results presented here are somewhat qualitative in nature. However, during the next pandemic, the real-time estimation of these key unknowns (a challenging task in itself) will constrain models such as those presented here, thus yielding quantitative, testable predictions.

Finally, we note that the present study also identifies several areas in which further research should be carried out. As is often the case with modeling studies, new empirical data are essential to further constrain and corroborate the models, particularly with regard to contact rates during times of social disruption, including school closures. We recognize that school dismissal incurs substantial economic and societal costs (in addition to removing a convenient location for implementing a childhood vaccination campaign), and a more complete economic analysis should be performed before recommending any specific policies. Several economic analyses of different policy options have been reported (Cauchemez et al., 2009; Halder et al., 2011; Brown et al., 2011; Milne et al., 2013; Nishiura et al., 2014), but a more comprehensive economic analysis of school closures as a pandemic mitigation strategy, both on its own and in conjunction with pandemic vaccination, would be helpful, as well as further consideration of societal options that may mitigate the secondary impact of school closures.

Supplementary Material

Refer to Web version on PubMed Central for supplementary material.

Acknowledgements

We gratefully acknowledge Martin Meltzer, Noreen Qualls, Jeanette Rainey, Stephen Redd, and David Swerdlow for their support and advice during this study.

This work was sponsored by the United States Centers for Disease Control and Prevention. Los Alamos National Laboratory, an affirmative action/equal opportunity employer, is operated by Los Alamos National Security, LLC, for the National Nuclear Security Administration of the United States Department of Energy under contract DE-AC52-06NA25396. Because this research did not involve human subjects, it was not subject to IRB review requirements.

References

Biggerstaff M, Jhung M, Kamimoto L, Balluz L, Finelli L, 2012. Self-reported influenza-like illness and receipt of influenza antiviral drugs during the 2009 pandemic, United States, 2009–2010. Am. J. Public Health 102, e21.

Biggerstaff M, et al. , 2015. Estimating the potential effects of a vaccine program against an emerging influenza pandemic—united States. Clin. Infect. Dis. 60 (suppl 1), S20–S29. [PubMed: 25878298]

Blower SM, Dowlatabadi H, 1994. Sensitivity and uncertainty analysis of complex-models of disease transmission – an HIV model, as an example. Int. Stat. Review 62, 229–243.

Brown ST, et al. , 2011. Would school closure for the 2009 H1N1 influenza epidemic have been worth the cost?: a computational simulation of Pennsylvania. BMC Public Health 11 (353).

Carrasco LR, Jit M, Chen MI, Lee VJ, Milne GJ, Cook AR, 2013. Trends in parameterization, economics and host behaviour in influenza pandemic modelling: a review and reporting protocol. Emerg. Themes Epi. 10, 3.

Cauchemez S, et al. , 2009. Closure of schools during an influenza pandemic. Lancet Infect. Dis. 9, 473–481. [PubMed: 19628172]

Centers for Disease Control and Prevention, 2007. Interim Pre-pandemic Planning Guidance: Community Strategy for Pandemic Influenza Mitigation in the United States - Early Targeted Layered Use of Non-pharmaceutical Interventions. http://www.flu.gov/planning-preparedness/community/community_mitigation.pdf.

Centers for Disease Control and Prevention, 2010. 2009 H1N1 Vaccine Doses Allocated, Ordered, and Shipped by Project Area. http://www.cdc.gov/h1n1flu/vaccination/vaccinesupply.htm.

Centers for Disease Control and Prevention, 2011. Antiviral agents for the treatment and chemoprophylaxis of influenza: recommendations of the advisory committee on immunization practices (ACIP). Morbidity and Mortality Weekly Report 60, 1–25. http://www.cdc.gov/mmwr/pdf/rr/rr6001.pdf.

Chao DL, Halloran ME, Longini IM, 2010. School opening dates predict pandemic influenza A(H1N1) outbreaks in the United States. J. Infect. Dis. 202, 877–880. [PubMed: 20704486]

Chowell G, et al. , 2011. Characterizing the epidemiology of the 2009 influenza A/H1N1 pandemic in Mexico. PLoS Med. 8, e1000436.

Copeland DL, et al. , 2013. Effectiveness of a school district closure for pandemic influenza a (H1N1) on acute respiratory illnesses in the community: a natural experiment. Clin. Infect. Dis. 56, 509–516. [PubMed: 23087391]

Cowling BJ, Fang VJ, Riley S, Malik Peiris JS, Leung GM, 2009. Estimation of the serial interval of influenza. Epidemiology 20, 344–347. [PubMed: 19279492]

De LuCa G, Kerckhove KV, Coletti P, Poletto C, Bossuyt N, Hens N, Colizza V, 2018. The impact of regular school closure on seasonal influenza epidemics: a data-driven spatial transmission model for Belgium. BMC Infect. Dis. 18.1, 29. [PubMed: 29321005]

Eames KT, Tilston NL, Brooks-Pollock E, Edmunds WJ, 2012. Measured dynamic social contact patterns explain the spread of H1N1v influenza. PLoS Comput. Biol. 8, e1002425.

Earn DJD, et al. , 2012. Effects of school closure on incidence of pandemic influenza in Alberta, Canada. Ann. Intern. Med. 156, 173–181. [PubMed: 22312137]

Fumanelli L, Ajelli M, Merler S, Ferguson NM, Cauchemez S, 2016. Model-based comprehensive analysis of school closure policies for mitigating influenza epidemics and pandemics. PLoS Comput. Biol. 12 (1) e1004681.

Fung IC-H, Gambhir M, Glasser JW, Gao H, Washington ML, Uzicanin A, Meltzer MI, 2015. Modeling the effect of school closures in a pandemic scenario: exploring two different contact matrices. Clin. Infect. Dis. 60 (suppl 1), S58–S63. [PubMed: 25878302]

Gerdil C, 2003. The annual production cycle for influenza vaccine. Vaccine 21, 1776–1779. [PubMed: 12686093]

Germann TC, Kadau K, Longini IM, Macken CA, 2006. Mitigation strategies for pandemic influenza in the United States. Proc. Natl. Acad. Sci. U.S.A. 103, 5935–5940. [PubMed: 16585506]

Gog JR, et al. , 2014. Spatial transmission of 2009 pandemic influenza in the US. PLoS Comput. Biol. 10, e1003635.

Haber MJ, et al. , 2007. Effectiveness of interventions to reduce contact rates during a simulated influenza pandemic. Emerg Infect Dis 13, 581–589. [PubMed: 17553273]

Halder N, Kelso JK, Milne GJ, 2010. Developing guidelines for school closure interventions to be used during a future influenza pandemic. BMC Infect. Dis. 10, 221. [PubMed: 20659348]

Halder N, Kelso JK, Milne GJ, 2011. Cost-effective strategies for mitigating a future influenza pandemic with H1N1 2009 characteristics. PLoS One 6, e22087.

Halloran ME, et al. , 2008. Modeling targeted layered containment of an influenza pandemic in the USA. Proc. Natl. Acad. Sci. U.S.A. 105, 4639–4644. [PubMed: 18332436]

Heymann A, Chodick G, Reichman B, Kokia E, Laufer J, 2004. Influence of school closure on the incidence of viral respiratory diseases among children and on health care utilization. Pediatr. Infect. Dis. J. 23, 675–677. [PubMed: 15247610]

Lee BY, et al. , 2010. Simulating school closure strategies to mitigate an influenza epidemic. J. Pub. Health Managmt. Practice 16, 252–261.

Lipsitch M, et al. , 2007. Antiviral resistance and the control of pandemic influenza. PLoS Med. 4, e15.

Longini IM, et al. , 1982. Estimating household and community transmission parameters for influenza. Am. J. Epidemiol. 115, 736–751. [PubMed: 7081204]

Longini IM, Halloran ME, Nizam A, et al. , 2000. Estimation of the efficacy of live, attenuated influenza vaccine from a two-year, multi-center vaccine trial: implications for influenza epidemic control. Vaccine 18, 1902–1909. [PubMed: 10699339]

Markel H, et al. , 2007. Nonpharmceutical interventions implemented by US cities during the 1918–1919 influenza pandemic. JAMA 298, 644–654. [PubMed: 17684187]

Milne GJ, Kelso JK, Kelly HA, Huband ST, McVernon J, 2008. A small community model for the transmission of infectious diseases: comparison of school closure as an intervention in individual-based models of an influenza pandemic. PLoS One 3, e4005.

Milne GJ, Halder N, Kelso JK, 2013. The cost effectiveness of pandemic influenza interventions: a pandemic severity based analysis. PLoS One 8, e61504.

Mossong J, et al. , 2008. Social contacts and mixing patterns relevant to the spread of infectious diseases. PLoS Med. 5, e74.

Nishiura H, et al. , 2014. Cost-effective length and timing of school closure during an influenza pandemic depend on the severity. Theor. Biol. Med. Model. 11, 5. [PubMed: 24447310]

President's Council of Advisors on Science and Technology, 2010. Report to the President on Reengineering the Influenza Vaccine Production Enterprise to Meet the Challenges of Pandemic Influenza. . https://www.whitehouse.gov/sites/default/files/microsites/ostp/PCAST-Influenza-Vaccinology-Report.pdf.

Reed C, et al. , 2009. Estimates of the prevalence of pandemic (H1N1) 2009, United States, April–July 2009. Emerg. Infect. Dis. 15, 2004–2007. [PubMed: 19961687]

Reed C, et al. , 2013. Novel framework for assessing epidemiologic effect of influenza epidemics and pandemics. Emerg. Infect. Dis. 19, 85–91. [PubMed: 23260039]

Riley S, 2007. Large-scale spatial-transmission models of infectious disease. Science 316 (1298).

Viboud C, et al. , 2004. Risk factors of influenza transmission in households. Br. J. Gen. Pract. 54, 684–689. [PubMed: 15353055]

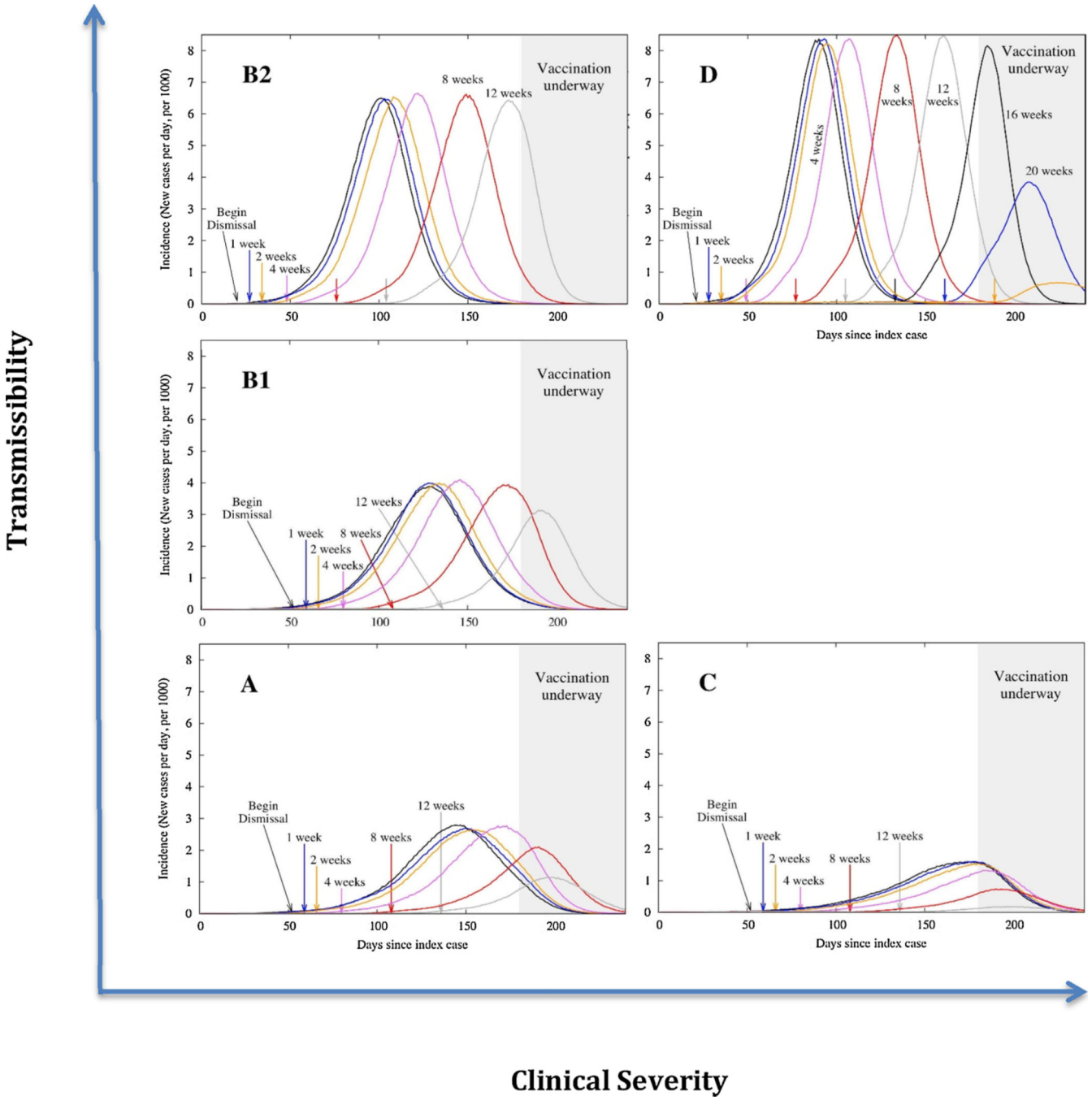

Fig. 1.

Effect of school dismissal duration upon epidemic curves for simultaneous (region-wide) school dismissal for the regional model (the Chicago metropolitan area, with 8.6 M people). Results are shown for the shorter serial interval and nominal (worst-case) contact rate changes upon dismissal, activated when 20 children are symptomatic in a community (i.e., closure upon the first diagnosed case if the diagnosis ratio is 5%). Results are shown for five pandemic scenarios: four historically referenced 20th century influenza pandemics (A: 2009,

B1:1968, B2: 1957, D: 1918) and a fifth scenario (C) that corresponds to a clinically severe but less transmissible pandemic.

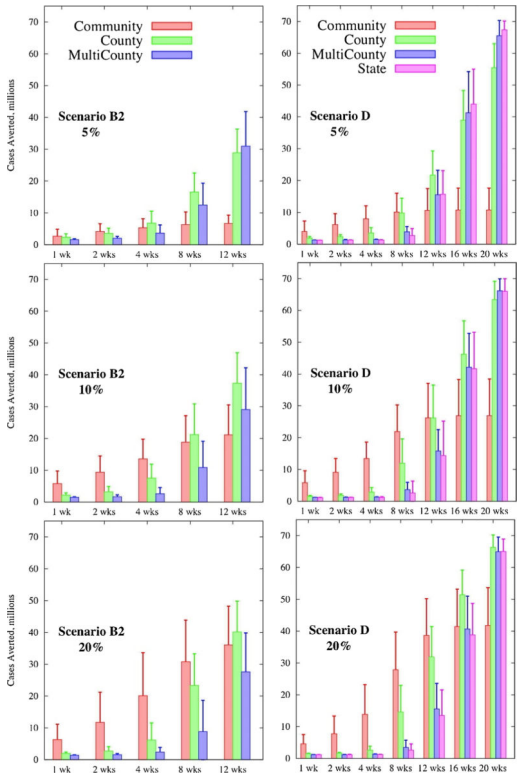

Fig. 2.

U.S. model predictions of the number of (symptomatic) influenza cases averted by a combination of self-isolation, school dismissals, and vaccination, for the shorter serial interval. School dismissal is activated when one symptomatic child is diagnosed at an assumed diagnosis ratio of 5%, 10%, or 20%. Two alternative assumptions for contact rates (CR) during school dismissal are considered: “worst-case” (filled bars: CR involving children in households are doubled and child-related contacts outside the home are reduced by 30%) and “best-case” (extensions: CR involving children in households are unchanged, and child-related contacts outside the home are reduced by 50%). Beginning on day 180, 1 million people per day are vaccinated (see text and SI for details).

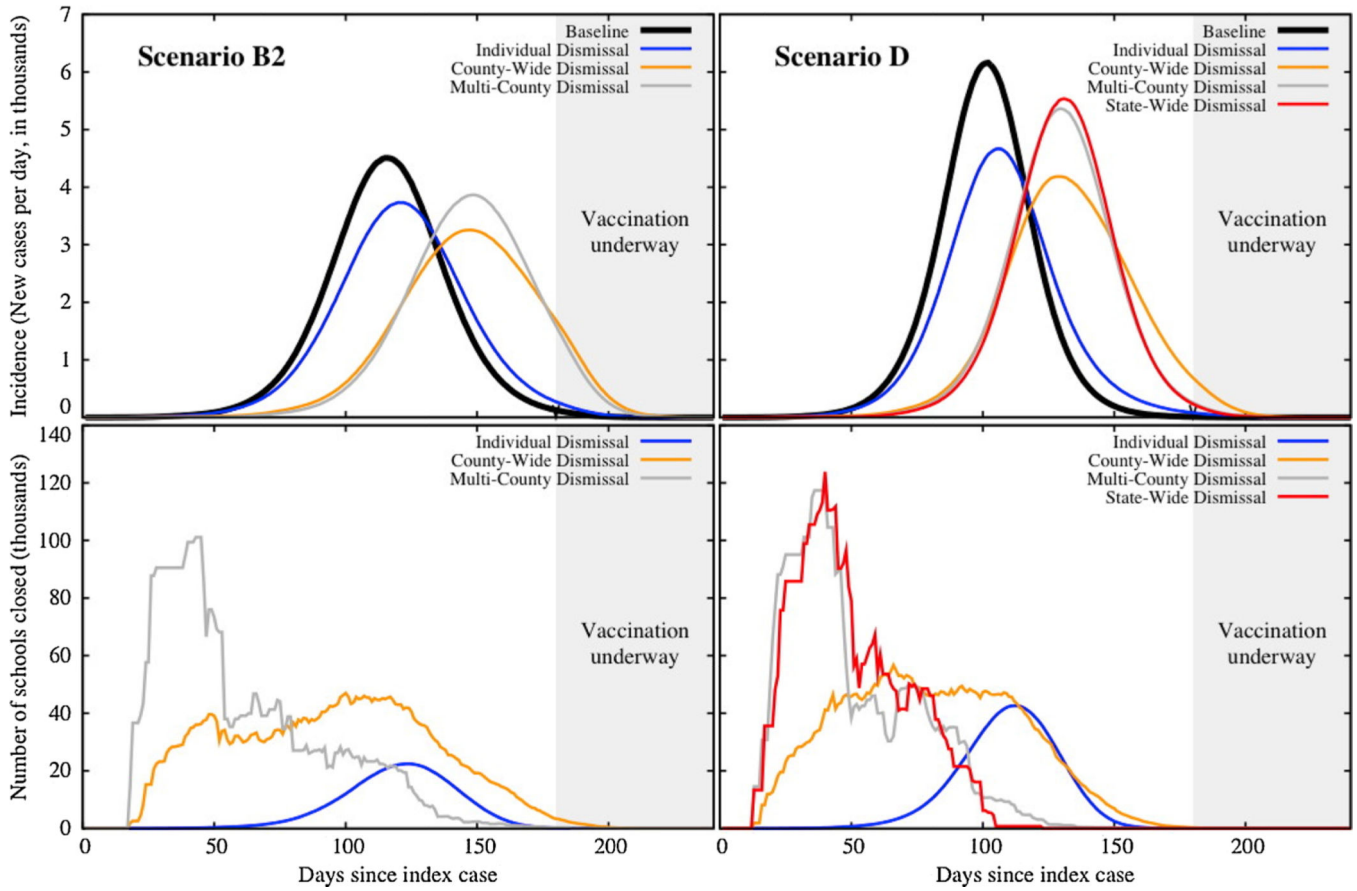

Fig. 3.

U.S. model results for pandemic scenarios B2 (left panels) and D (right panels). School dismissal activated when 20 children are symptomatic (closure upon first diagnosed at a 5% diagnosis ratio) and a 4-week duration, for the shorter serial interval. (Top) Epidemic curves. (Bottom) Number of schools closed at any time during the outbreak. The “worst-case” assumption for contact rates during school dismissal is used (contact rates involving children in households are doubled, and child-related contacts outside the home are reduced by 30%). Analogous results for the “best-case” contact rates are shown in Fig. S6. Beginning on day 180, 1 million people per day are vaccinated (see text and SI for details). Note that for scenario D, the multi-county and state-wide dismissals are virtually indistinguishable, particularly for the epidemic curves.

Table 1

Summary of key EpiCast model parameters for this study (see Supporting Online Material and Germann et al (Germann et al., 2006) for further details).

Parameter	Options	Key attributes		
Pandemic scenario[a]	A(2009 like)	18% (32%, 15%, 7%), 1.3		Overall and age-specific (child, adult, elderly[b]) attack rates and R_0
	B1(1968 like)	22% (39%, 18%, 8%), 1.5		
	B2(1957 like)	28% (50%, 23%, 11%), 1.8		
	C(H5N1 like)	10% (18%, 8%, 4%), 1.2		
	D(1918 like)	30% (54%, 25%, 12%), 2.0		
Serial interval[c]	Short	1.98, 1.98, 1.61 days		Mean latent, incubation, and infectious period durations
	Long	1.2, 1.9, 4.1 days		
School dismissal trigger[d]	1%	100	Diagnosis ratio[c] (percentage of symptomatic individuals correctly identified) and corresponding number of symptomatic schoolchildren in a community required to trigger dismissal	
	5%	20		
	10%	10		
	20%	5		
School dismissal duration	1, 2, 4, 8, and 12 weeks		and 16, 20, 24 weeks for scenario D	
School dismissal geographic scale	Community		For regional model: Community or Regional	
	County			
	Multi-county			
	State			
Child-related contact changes during dismissal	Worst-case	100% increase in child-related household contacts		
		30% reduction in child-related non-household contacts		
	Best-case	No change in child-related household contacts		
		50% reduction in child-related non-household contacts		

[a] Pandemic scenarios are based on a two-dimensional framework recently developed by (Reed et al. (2013)).

[b] Ages 0–18 years are considered children, 19–64 adult, and 65+ years elderly.

[c] The serial interval, or generation time, is the interval between successive cases in a chain of transmission.

[d] School dismissal is triggered when the first confirmed symptomatic school-age child is detected in a community. The diagnosis ratio is the percentage of symptomatic individuals that are positively identified; for instance, with a 5% diagnosis ratio, the first confirmed case may not be identified until 20 children are symptomatic.

Table 2:

Cumulative attack rates (AR) with the reduction from the baseline scenario in parentheses (δ) using the regional model, with the shorter (mean ~2.8 day) serial interval and best-case contact pattern change (a 50% reduction in non-household contacts) during school dismissal. Analogous tables for the longer serial interval and/or worst-case contact patterns are provided in the SI.

Pandemic scenario	Baseline Clinical Attack Rate[a]	Trigger	Community School Dismissal[c]					Regional School Dismissal[c]				
		Diag. ratio[b]	Duration					Duration				
			1 wk AR(δ)	2 wks AR(δ)	4 wks AR(δ)	8 wks AR(δ)	12 wks AR(δ)	1 wk AR(δ)	2 wks AR(δ)	4 wks AR(δ)	8 wks AR(δ)	12 wks AR(δ)
A (2009-like)	18.4%	1%	18.4 (0.0)	18.4 (0.0)	18.4 (0.0)	18.4 (0.0)	18.4 (0.0)	18.4 (0.0)	18.4 (0.0)	18.4 (0.0)	18.4 (0.0)	18.4 (0.0)
		5%	17.1 (1.3)	16.6 (1.8)	16.4 (2.1)	16.2 (2.2)	16.1 (2.3)	17.9 (0.5)	17.3 (1.1)	14.9 (3.5)	8.2 (10.2)	3.0 (15.4)
		10%	14.6 (3.8)	12.8 (5.6)	11.8 (6.6)	10.9 (7.5)	10.5 (7.9)	18.1 (0.4)	17.4 (1.0)	15.0 (3.4)	9.7 (8.7)	4.5 (13.9)
		20%	12.5 (5.9)	8.4 (10.0)	6.0 (12.4)	5.0 (13.4)	4.5 (13.9)	17.9 (0.5)	17.1 (1.3)	15.9 (2.5)	10.7 (7.7)	5.0 (13.4)
B1 (1968-like)	22.6%	1%	22.6 (0.0)	22.6 (0.0)	22.6 (0.0)	22.6 (0.0)	22.6 (0.0)	22.6 (0.0)	22.6 (0.0)	22.6 (0.0)	22.6 (0.0)	22.6 (0.0)
		5%	21.1 (1.5)	20.6 (2.0)	20.2 (2.4)	19.7 (2.9)	19.5 (3.0)	22.5 (0.1)	22.3 (0.3)	21.6 (1.0)	15.6 (7.0)	7.9 (14.7)
		10%	19.4 (3.2)	17.9 (4.6)	16.3 (6.3)	14.2 (8.4)	13.3 (9.3)	22.5 (0.1)	22.4 (0.2)	21.7 (0.9)	17.2 (5.3)	9.6 (13.0)
		20%	18.9 (3.7)	16.0 (6.6)	12.6 (10.0)	9.2 (13.4)	7.5 (15.0)	22.5 (0.1)	22.4 (0.2)	22.0 (0.6)	18.3 (4.3)	10.5 (12.0)
B2 (1957-like)	28.3%	1%	28.3 (0.0)	28.3 (0.0)	28.3 (0.0)	28.3 (0.0)	28.3 (0.0)	28.3 (0.0)	28.3 (0.0)	28.3 (0.0)	28.3 (0.0)	28.3 (0.0)
		5%	25.6 (2.7)	24.5 (3.8)	23.3 (5.0)	22.0 (6.4)	21.4 (6.9)	28.3 (0.1)	28.3 (0.0)	28.2 (0.1)	27.0 (1.3)	19.7 (8.7)
		10%	25.2 (3.1)	23.8 (4.5)	21.5 (6.9)	16.7 (11.6)	14.0 (14.4)	28.2 (0.1)	28.3 (0.0)	28.2 (0.1)	27.2 (1.1)	20.7 (7.6)
		20%	26.2 (2.1)	24.8 (3.5)	21.5 (6.8)	14.6 (13.7)	9.4 (18.9)	28.3 (0.0)	28.3 (0.1)	28.2 (0.1)	27.5 (0.8)	22.4 (5.9)
C (H5Nl-like)	12.1%	1%	12.1 (0.0)	12.1 (0.0)	12.1 (0.0)	12.1 (0.0)	12.1 (0.0)	12.1 (0.0)	12.1 (0.0)	12.1 (0.0)	12.1 (0.0)	12.1 (0.0)
		5%	11.5 (0.6)	11.1 (1.0)	11.0 (1.1)	11.1 (1.0)	11.1 (1.0)	11.0 (1.1)	9.5 (2.6)	6.2 (5.9)	2.8 (9.3)	0.9 (11.2)
		10%	9.1 (3.0)	7.7 (4.4)	7.0 (5.1)	6.9 (5.2)	6.9 (5.2)	11.2 (0.9)	10.0 (2.1)	7.2 (4.9)	3.8 (8.3)	1.4 (10.7)
		20%	6.4 (5.7)	3.7 (8.4)	3.0 (9.1)	2.7 (9.4)	2.4 (9.7)	11.5 (0.6)	9.9 (2.2)	8.2 (3.9)	4.4 (7.7)	1.8 (10.3)
D (1918-like)	30.1%	1%	30.1 (0.0)	30.1 (0.0)	30.1 (0.0)	30.1 (0.0)	30.1 (0.0)	29.7 (0.4)	29.5 (0.6)	29.1 (1.0)	27.3 (2.8)	24.7 (5.4)
		5%	26.8 (3.3)	25.5 (4.6)	24.0 (6.1)	21.5 (8.6)	20.6 (9.5)	30.1 (0.0)	30.1 (0.0)	30.1 (0.0)	30.0 (0.1)	27.0 (3.1)
		10%	27.3 (2.8)	26.3 (3.8)	25.0 (5.1)	19.3 (10.8)	14.1 (16.0)	30.1 (0.0)	30.1 (0.0)	30.1 (0.0)	30.0 (0.1)	27.8 (2.3)
		20%	28.5 (1.6)	27.9 (2.2)	26.9 (3.2)	21.5 (8.6)	12.4 (17.7)	30.1 (0.0)	30.1 (0.0)	30.1 (0.0)	30.0 (0.1)	28.4 (1.7)

[a] Cumulative clinical attack rates (i.e., the percentage of the total population who develop clinical symptoms within 240 days of the index case, i.e. including 60 days after the vaccination campaign has started) are given for the baseline (no dismissal) scenario and various school dismissal policy options.

[b] School dismissal is triggered when the first confirmed symptomatic school-age child is detected in a community. The diagnosis ratio is the percentage of symptomatic individuals that are positively identified; for instance, with a 5% diagnosis ratio, the first confirmed case may not be identified until 20 children are symptomatic.

[c] Upon triggering a dismissal, either only the affected community's schools are closed (community dismissal) or a simultaneous dismissal of all Chicago-area schools (regional dismissal).